

The moving-grid effect in density functional calculations of harmonic vibration frequencies using numeric atom-centered grids

Honghui Shang^{1, a)}

Fritz-Haber-Institut der Max-Planck-Gesellschaft, Faradayweg 4-6, D-14195 Berlin-Dahlem, Germany

(Dated: 12 August 2018)

When using atom-centered integration grids, the portion of the grid that belongs to a certain atom also moves when this atom is displaced. In the paper, we investigate the moving-grid effect for harmonic vibrational frequencies for all-electron full-potential numeric basis set calculation. We found that, unlike the first derivatives (i.e., forces), this moving-grid effect plays an essential role for second derivatives (i.e., vibrational frequencies). Further analysis reveals that predominantly diagonal force constant terms are affected, which can be bypassed efficiently by invoking translational symmetry.

PACS numbers: 71.15.-m

I. INTRODUCTION

Density-functional theory (DFT)^{1,2} has been developed into a widely applied ground-state method for polyatomic systems in chemistry, physics and material science. In addition, the response properties (e.g., polarizability, vibrational frequencies or phonon dispersions) related to the derivatives of the total energy can be calculated within the same quantum mechanical framework by means of density-functional perturbation theory (DFPT)³⁻⁵ or so-called coupled perturbed self-consistent field (CPSCF) method⁶⁻¹¹ in quantum chemistry community. The popularizing of DFT in quantum chemistry community came from an excellent paper by Johnson, Gill and Pople¹², in which they systematically studied the performance (optimized geometries, dipole moments, vibrational frequencies and atomization energies) of a number of different density functionals. In this paper, they also mentioned that in the calculation of exchange-correlation energy gradient, the positions of the grid points are a central feature in the definition of the numerical exchange-correlation energy, which can be integrated numerically using different kinds of grids. One naturally choice is the uniform grid which has been used in many DFT software, e.g., OCTOPUS¹³, SIESTA¹⁴. Another kind of grid is the atom-centered grid, which is defined such that an atom's grid "moves with" a displacement of its nucleus. Such atom-centered grid was first proposed by Satoko¹⁵ and then developed by Becke¹⁶. The advantage of the atom-centered grid are three-fold, firstly it could treat full-electron system where the integrand is dominated by cusps at atomic nuclei; secondly multicenter Poisson's equation can be reduced to a set of independent one-center Poisson's equations. Thirdly, such atomic-center-partition scheme can bypass so-called egg-box effect¹⁴ as shown in uniform grids. Thanks to the above advantages, such atomic-center grid has been

widely adopted in the implementation of DFT in quantum chemistry software since 1990s¹⁷⁻¹⁹.

However, this atomic partition scheme suffers from so-called moving-grid effect when derivatives are needed. This is because when an atom moves, all the points belong to this atom also move with it, for example, in Fig. (1), the hydrogen atom labeled as H_J is moved to the right side, so the grids belong to this atom are also moved (see $H_{J,after}$), on the contrary, the grids belong to atom hydrogen H_I are kept as before (see $H_{I,after}$); In addition, the integration weight functions are also changed, so the derivatives of the weight function need to be included, as shown in Fig. 2), when the hydrogen atom labeled as H_J is moved to the right side, the weight functions of both atom H_J and H_I are changed. We call the above two phenomena as moving-grid effect. When the derivatives of the exchange-correlation energy are calculated using Gaussian basis set, this moving-grid effect (or called effect of quadrature weight derivatives in the previous literature^{18,20}) has been found to be important for both force and Hessian when grids are insufficient quality.^{12,20,21}

Moreover, when numerical basis set is used, both the Coulomb terms and the exchange-correlation term needs numerical integration¹⁷. So in principle, this moving-grid effect using numerical basis set could be more serious than using Gaussian basis set which treats Coulomb terms analytically. In 1991, Delley made a first analytical energy derivative implementation using numerical basis set, in Ref.¹⁷, he also mentioned that for first-order derivative calculation, the moving-grid effect only "results in a small residual (e.g., 10^{-3} a.u.) at the energy minimum", which could be left out in his opinion. However, how about its influence on the second-order derivatives (force constant/Hessian)? To the best of our knowledge, until now, it is still unknown when using atom-centered numerical basis set.

Recently, we completed our implementation²² of density-functional perturbation theory (DFPT) for harmonic vibrational properties in molecules and solids, using numeric atom-centered orbitals as basis func-

^{a)}Electronic address: shang@fhi-berlin.mpg.de

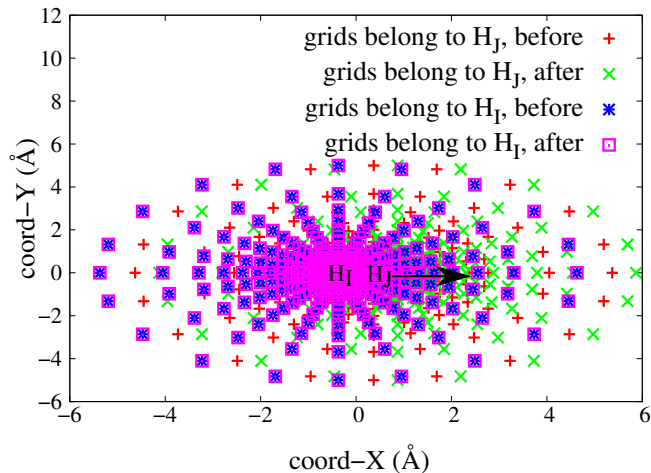


FIG. 1. The coordinates (X and Y, with $Z=0$ Å) of atom-centered grid for H_2 molecule. The atom H_I is fixed and the atom H_J is moved to the right side with 0.5 Å as shown by arrow. Here we show the atom-centered grids for H_2 molecule both before and after atom H_J is moved.

tions (discussed exemplarily for the all-electron Fritz Haber Institut *ab initio* molecular simulations (FHI-aims) package²³.) Here we will show the moving-grid effect in second-order derivative calculation when using such atom-centered numerical basis set. We find that, unlike for first derivatives (i.e. forces), this moving-grid effect plays an important role for second derivatives (i.e. vibrational frequencies). We only discussed molecule in this paper. And in order to keep the same line as Delley¹⁷, the screened scheme^{22,23} is not used for Hellman-Feynman force and Hessian calculation. In fact, when using screened scheme, the moving-grid effect for Hellman-Feynman force could be bypassed as the derivative in screened scheme is analytically gotten, so the moving-grid effect only appeared in Pulay-force calculation. So does the force constants/Hessian calculation.

The remainder of the paper is organized as follows. In Sec. II, we gave the fundamental theoretical framework. In section III, the results for diatomic H_2 , F_2 , Cl_2 will be given by using a variety of basis set a different dense of grids. Eventually, Sec. IV summarizes the main ideas and findings of this work.

II. METHOD

A. Integration scheme

Our approach for atom-centered integration grid²³ is similar to the one developed by Delley^{20,24,25}. Firstly, the grids are partitioned to each atoms using partition function defined^{23,24} as

$$p_I(\mathbf{r}) = \frac{g_I(\mathbf{r})}{\sum_{I'} g_{I'}(\mathbf{r})}, \quad (1)$$

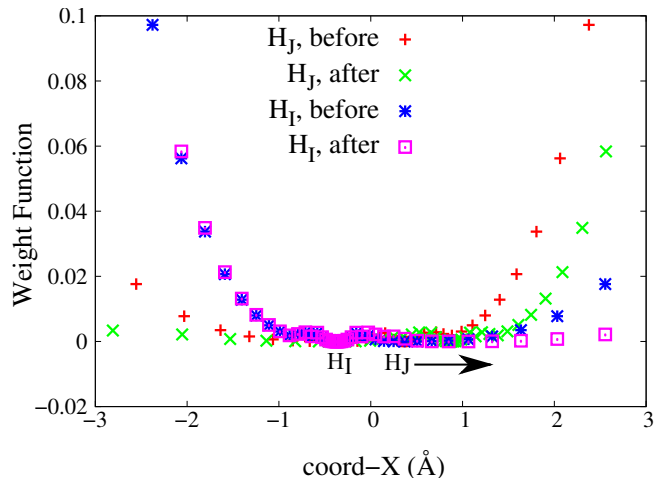


FIG. 2. The weight function $w(\mathbf{r})$ (at $Y=0$ Å and $Z=0$ Å) with respect to X coordinate for H_2 molecule. The atom H_I is fixed and the atom H_J is moved to the right side with 0.5 Å as shown by arrow. We could see the weight function of grids both belong to atom H_I and H_J are changed.

here g_I is a peaked function, we use Delley's²⁴ approach in this paper.

$$g_I(\mathbf{r}) = \frac{n_I^{free}(|\mathbf{r} - \mathbf{R}_I|)}{|\mathbf{r} - \mathbf{R}_I|^2}, \quad (2)$$

where n_I^{free} is the electron density of free atoms. For each atom, radially the atom-centered grid consists of N_r spherical integration shells, the outermost of which lies at a distance r_{outer} from the nucleus. The shell density can be controlled by means of the radial multiplier $N_{r,mult}$. For example, $N_{r,mult}=2$ results in a total of $2N_r + 1$ radial integration shells, with radial integration weight $w_{rad}(s)$ ^{20,23}. On these shells, angular integration points are distributed in such a way that spherical harmonics up to a certain order are integrated exactly by the use the Lebedev grids proposed by Delley²⁵, with angular integration weights $w_{ang}(t)$. Then we could have weight function $w(\mathbf{r})$ for grids belong to atom I:

$$w_I(\mathbf{r}) = p_I(\mathbf{r})w_{rad}(s)w_{ang}(t), \quad (3)$$

and the derivative of weight function :

$$\frac{dw_I(\mathbf{r})}{d\mathbf{R}_J} = \frac{dp_I(\mathbf{r})}{d\mathbf{R}_J} w_{rad}(s)w_{ang}(t), \quad (4)$$

where the derivative of partition function $p_I(\mathbf{r})$ is

$$\begin{aligned} \frac{dp_I(\mathbf{r})}{d\mathbf{R}_J} = & -(1 - \delta_{IJ}) \frac{g_I(\mathbf{r})}{[\sum_{I'} g_{I'}(\mathbf{r})]^2} \frac{dg_J(\mathbf{r})}{d\mathbf{R}_J} \\ & - \delta_{IJ} \frac{g_I(\mathbf{r})}{[\sum_{I'} g_{I'}(\mathbf{r})]^2} \sum_{I' \neq I} \frac{dg_{I'}(\mathbf{r})}{d\mathbf{R}_I}, \end{aligned} \quad (5)$$

here $\delta_{I,J}$ denotes Kronecker delta.

In practical implementation, the integrals in total energy (force, force constants) are not calculated analytically, but approximated by a discrete summation:

$$\begin{aligned} Int &= \int d\mathbf{r} f(\mathbf{r}, \mathbf{R}) \\ &\approx \sum_I \sum_{\mathbf{r}} w_I(\mathbf{r}) f(\mathbf{r}, \mathbf{R}_I), \end{aligned} \quad (6)$$

and the derivative of this integrals is

$$\begin{aligned} \frac{dInt}{d\mathbf{R}_J} &\approx \sum_I \sum_{\mathbf{r}} \frac{\partial w_I(\mathbf{r})}{\partial \mathbf{R}_J} f(\mathbf{r}, \mathbf{R}_I) \\ &+ \sum_I \sum_{\mathbf{r}} w_I(\mathbf{r}) \frac{df(\mathbf{r}, \mathbf{R}_I)}{d\mathbf{R}_J}. \end{aligned} \quad (7)$$

The moving-grid effect appears in the derivative calculation (Eq.7), which is needed in the force and force constants calculation. As shown in Ref.²⁰, for force calculation, essentially identical results could be obtained with the moderate size grids (around 3500 points per atom) whether or not moving-grid effect are considered. In FHI-aims, even the smallest grid sizes (light setting) is around 5000 grid points per atom, so in this paper, we have not considered the moving-grid effect in the force calculation, but only for the force constants.

B. Force and force constants

In FHI-aims²³, the force which is the first-order derivative of the total energy (E_{tot}) can be split into three terms

$$\vec{F}_I = -\frac{dE_{tot}}{d\mathbf{R}_I} = \vec{F}_I^{HF} + \vec{F}_I^P + \vec{F}_I^{MP}. \quad (8)$$

The Hellmann-Feynman force in a screened form is written as

$$\vec{F}_I^{HF} = Z_I \left(\frac{\partial V_I^{es}(0)}{\partial \mathbf{R}_I} + \sum_{J \neq I} \frac{\partial V_J^{es,tot}(|\mathbf{R}_I - \mathbf{R}_J|)}{\partial \mathbf{R}_I} \right), \quad (9)$$

in which V_I^{es} refers to the electronic Hartree potential, and $V_I^{es,tot}$ refers to the total electronic potential, i.e., the electronic Hartree potential screened by the nuclear external potential^{22,23}. In a more explicit form, the Hellmann-Feynman term can be written as

$$\vec{F}_I^{HF} = - \int n(\mathbf{r}) \frac{Z_I(\mathbf{R}_I - \mathbf{r})}{|\mathbf{r} - \mathbf{R}_I|^3} d\mathbf{r} + \sum_{J \neq I} \frac{Z_I Z_J (\mathbf{R}_I - \mathbf{R}_J)}{|\mathbf{R}_I - \mathbf{R}_J|^3}. \quad (10)$$

It should be noted that, by default in FHI-aims, the Hellman-Feynman force is calculated using Eq.(9). Here we write down Eq.(10) in order to keep the same form as Delley¹⁷. The other reason is that in the screened form as shown in Eq.(9), the Hellman-Feynman part could be gotten analytically, and the moving-grid effect could not be shown.

The Pulay force can be written with expansion coefficients $C_{\mu i}$ and atomic basis set $\chi_{\mu}(\vec{r})$

$$\vec{F}_I^P = -2 \sum_{i,\mu,\nu} f_i C_{\mu i}^* C_{\nu i} \int \frac{\partial \chi_{\mu}(\mathbf{r})}{\partial \mathbf{R}_I} (\hat{h}_{KS} - \epsilon_i) \chi_{\nu}(\mathbf{r}) d\mathbf{r}, \quad (11)$$

where the Hamiltonian is $\hat{h}_{KS} = \hat{t}_s + \hat{v}_{ext}(r) + \hat{v}_H + \hat{v}_{xc}$, and the force arising from the multipole correction is

$$\vec{F}_I^{MP} = - \int (n(\mathbf{r}) - n^{MP}(\mathbf{r})) \frac{\partial V_I^{es,tot}(\mathbf{r} - \vec{R}_I)}{\partial \mathbf{R}_I} d\mathbf{r}. \quad (12)$$

The Pulay term can be rewritten as

$$\begin{aligned} \vec{F}_I^P &= -2 \sum_{\mu\nu} P_{\mu\nu} \int \frac{\partial \chi_{\mu}(\mathbf{r})}{\partial \mathbf{R}_I} \hat{h}_{ks} \chi_{\nu}(\mathbf{r}) d\mathbf{r} \\ &+ 2 \sum_{\mu\nu} W_{\mu\nu} \int \frac{\partial \chi_{\mu}(\mathbf{r})}{\partial \mathbf{R}_I} \chi_{\nu}(\mathbf{r}) d\mathbf{r}, \end{aligned} \quad (13)$$

with density matrix

$$P_{\mu\nu} = \sum_i f_i C_{\mu i} C_{\nu i}, \quad (14)$$

and energy weighted density matrix

$$W_{\mu\nu} = \sum_i f_i \epsilon_i C_{\mu i} C_{\nu i}, \quad (15)$$

in which f_i denotes the occupation number of eigenstate.

Using the above form, we have force constants,

$$\Phi_{I,J} = \frac{d^2 E_{tot}}{d\mathbf{R}_I d\mathbf{R}_J} = \Phi_{IJ}^{HF} + \Phi_{IJ}^P. \quad (16)$$

Please note that we have omitted the multipole term here, since its contribution is already three orders of magnitude smaller at the level of the forces. For the sake of readability, its total derivative of the Hellman-Feynman term $\Phi_{I\alpha,J\beta}^{HF}$ is divided in to two terms

$$\Phi_{I,J}^{HF} = \Phi_{I,J}^{HF-r} + \Phi_{I,J}^{HF-R}. \quad (17)$$

Then the first term which is the derivative of the first term of Eq.(10), accounts for the response of the integration.

$$\begin{aligned} \Phi_{I,J}^{HF-r} &= \int \frac{\partial n(\mathbf{r})}{\partial \mathbf{R}_J} V_I^{(1)}(\mathbf{r}) d\mathbf{r} \\ &+ \int n(\mathbf{r}) \frac{\partial V_I^{(1)}}{\partial \mathbf{R}_J} d\mathbf{r}. \end{aligned} \quad (18)$$

If label the derivative of electron-ionic interaction as $V_I^{(1)}(\mathbf{r})$

$$V_I^{(1)}(\mathbf{r}) = \frac{Z_I(\mathbf{R}_I - \mathbf{r})}{|\mathbf{r} - \mathbf{R}_I|^3}, \quad (19)$$

and second order derivative of electron-ionic interaction is (with α and β label the coordinates)

$$\begin{aligned} \frac{\partial V_{I\alpha}^{(1)}(\mathbf{r})}{\partial \mathbf{R}_{J\beta}} &= \delta_{IJ} \delta_{\alpha\beta} \frac{Z_I}{|\mathbf{r} - \mathbf{R}_I|^3} \\ &- 3 \cdot \delta_{IJ} \frac{Z_I(\mathbf{R}_I - \mathbf{r})_{\alpha} (\mathbf{R}_J - \mathbf{r})_{\beta}}{|\mathbf{r} - \mathbf{R}_I|^5}. \end{aligned} \quad (20)$$

The second term

$$\begin{aligned} \Phi_{I\alpha,J\beta}^{HF-R} = & (1 - \delta_{IJ}) \left[\delta_{\alpha\beta} \frac{Z_I Z_J}{|\mathbf{R}_I - \mathbf{R}_J|^3} \right. \\ & \left. - 3 \cdot \frac{Z_I Z_J (\mathbf{R}_I - \mathbf{R}_J)_\alpha (\mathbf{R}_I - \mathbf{R}_J)_\beta}{|\mathbf{R}_I - \mathbf{R}_J|^5} \right] \\ & + \delta_{IJ} \left[-\delta_{\alpha\beta} \frac{Z_I Z_J}{|\mathbf{R}_I - \mathbf{R}_J|^3} \right. \\ & \left. + 3 \cdot \frac{Z_I Z_J (\mathbf{R}_I - \mathbf{R}_J)_\alpha (\mathbf{R}_I - \mathbf{R}_J)_\beta}{|\mathbf{R}_I - \mathbf{R}_J|^5} \right], \quad (21) \end{aligned}$$

accounts for the response of the ionic-ionic summation.

Similarly, the total derivative of Pulay term $\Phi_{I,J}^P$ is split into four terms:

$$\Phi_{I,J}^P = \Phi_{I,J}^{P-P} + \Phi_{I,J}^{P-H} + \Phi_{I,J}^{P-W} + \Phi_{I,J}^{P-S}. \quad (22)$$

The first term

$$\Phi_{I,J}^{P-P} = 2 \sum_{\mu,\nu} \left(\frac{dP_{\mu,\nu}}{d\vec{R}_J} \right) \int \frac{\partial \chi_\mu(\mathbf{r})}{\partial \mathbf{R}_I} \hat{h}_{KS} \chi_\nu(\mathbf{r}) d\mathbf{r}, \quad (23)$$

accounts for the response of the density matrix $P_{\mu,\nu}$. The second term

$$\begin{aligned} \Phi_{I,J}^{P-H} = & 2 \sum_{\mu,\nu} P_{\mu,\nu} \cdot \\ & \left(\int \frac{\partial^2 \chi_\mu(\mathbf{r})}{\partial \mathbf{R}_I \partial \mathbf{R}_J} \hat{h}_{KS} \chi_\nu(\mathbf{r}) d\mathbf{r} \right. \\ & + \int \frac{\partial \chi_\mu(\mathbf{r})}{\partial \mathbf{R}_I} \frac{d\hat{h}_{KS}}{d\vec{R}_J} \chi_\nu(\mathbf{r}) d\mathbf{r} \\ & \left. + \int \frac{\partial \chi_\mu(\mathbf{r})}{\partial \mathbf{R}_I} \hat{h}_{KS} \frac{\partial \chi_\nu(\mathbf{r})}{\partial \vec{R}_J} d\mathbf{r} \right), \quad (24) \end{aligned}$$

accounts for the response of the Hamiltonian $\hat{h}_{ks}(\vec{k})$, while the third and fourth term

$$\begin{aligned} \Phi_{I,J}^{P-W} = & -2 \sum_{\mu,\nu} \frac{dW_{\mu,\nu}}{d\vec{R}_J} \int \frac{\partial \chi_\mu(\mathbf{r})}{\partial \mathbf{R}_I} \chi_\nu(\mathbf{r}) d\mathbf{r} \quad (25) \\ \Phi_{I,J}^{P-S} = & -2 \sum_{\mu,\nu} W_{\mu,\nu} \left(\int \frac{\partial^2 \chi_\mu(\mathbf{r})}{\partial \mathbf{R}_I \partial \mathbf{R}_J} \chi_\nu(\mathbf{r}) \right. \\ & \left. + \int \frac{\partial \chi_\mu(\mathbf{r})}{\partial \mathbf{R}_I} \frac{\partial \chi_\nu(\mathbf{r})}{\partial \vec{R}_J} d\mathbf{r} \right), \quad (26) \end{aligned}$$

for the response of the energy weighted density matrix $W_{\mu,\nu}$ and the overlap matrix $S_{\mu,\nu}$, respectively. Please note that in all four contributions many terms vanish due to the fact that the localized atomic orbitals $\chi_\mu(\vec{r})$ are which implies, e.g.,

$$\frac{\partial \chi_\mu(\vec{r})}{\partial \vec{R}_J} = \frac{\partial \chi_\mu(\vec{r})}{\partial \vec{R}_J} \delta_{I(\mu),J}. \quad (27)$$

Similarly, it is important to realize that all partial derivatives that appear in the force constants can be readily computed numerically, since the $\chi_{\mu m}$ are numeric atomic orbitals, which are defined using a splined radial function and spherical harmonics for the angular dependence²³.

C. Moving-grid effect in force constants calculation

In force constants calculation, the moving-grid effect only appears the terms that contain integration. For Hellman-Feynman term, only $\Phi_{I\alpha,J\beta}^{HF-r}$ (Eq.18) need to be considered. For Pulay term, only $\Phi_{I,J}^{P-H}$ (Eq.24) and $\Phi_{I,J}^{P-S}$ (Eq.26) are considered. We will show in detail in the following section. The Hessian for exchange-correlation part is already inside Pulay hessian.

In the following, we will show our moving-grid scheme for the corresponding Hellman-Feynman term and Pulay term.

1. Moving-grid effect in Hellman-Feynman term

The $\Phi_{I,J}^{HF-r}$ (Eq.18) term is an integration, and we need use the approximation as shown in Eq.(7).

$$\begin{aligned} \Phi_{I,J}^{HF-r} \approx & \sum_{\mathbf{r}} \frac{\partial w(\mathbf{r})}{\partial \mathbf{R}_J} n(\mathbf{r}) V_I^{(1)}(\mathbf{r}) \\ & + \sum_{\mathbf{r}} w(\mathbf{r}) \left[\frac{\partial n(\mathbf{r})}{\partial \mathbf{R}_J} V_I^{(1)}(\mathbf{r}) + n(\mathbf{r}) \frac{\partial V_I^{(1)}(\mathbf{r})}{\partial \mathbf{R}_J} \right] \quad (28) \end{aligned}$$

Here first order density is

$$\begin{aligned} \frac{\partial n(\mathbf{r})}{\partial \mathbf{R}_J} = & \sum_{\mu\nu} \frac{\partial P_{\mu\nu}}{\partial \vec{R}_J} \chi_\mu(\vec{r}) \chi_\nu(\vec{r}) \\ & + \sum_{\mu\nu} P_{\mu\nu} \frac{\partial \chi_\mu(\vec{r})}{\partial \vec{R}_J} \chi_\nu(\vec{r}) \\ & + \sum_{\mu\nu} P_{\mu\nu} \chi_\mu(\vec{r}) \frac{\partial \chi_\nu(\vec{r})}{\partial \vec{R}_J}. \quad (29) \end{aligned}$$

When considering moving-grid effect, the derivative of basis function is written as:

$$\frac{\partial \chi_\mu(\vec{r})}{\partial \vec{R}_J} = \begin{cases} -\nabla \chi_\mu(\vec{r}) \delta_{I(\mu),J} & \text{if } \mathbf{r} \notin \text{atom}_J \\ \nabla \chi_\mu(\vec{r}) (1 - \delta_{I(\mu),J}) & \text{if } \mathbf{r} \in \text{atom}_J \end{cases} \quad (30)$$

and the electron-ionic interaction is

$$\frac{\partial V_I^{(1)}(\mathbf{r})}{\partial \vec{R}_J} = \begin{cases} \text{Eq.(20)} & \text{if } \mathbf{r} \notin \text{atom}_J \\ \text{Eq.(32)} & \text{if } \mathbf{r} \in \text{atom}_J \end{cases} \quad (31)$$

When r belong to atom_J , then it is moving grid, and the derivative of electron-ionic interaction is

$$\begin{aligned} \frac{\partial V_{I\alpha}^{(1)}(\mathbf{r})}{\partial \mathbf{R}_{J\beta}} = & -(1 - \delta_{IJ}) \delta_{\alpha\beta} \frac{Z_I}{|\mathbf{r} - \mathbf{R}_I|^3} \\ & + 3 \cdot (1 - \delta_{IJ}) \frac{Z_I (\mathbf{R}_I - \mathbf{r})_\alpha (\mathbf{R}_J - \mathbf{r})_\beta}{|\mathbf{r} - \mathbf{R}_I|^5}. \quad (32) \end{aligned}$$

2. Moving-grid effect in Pulay term

Similarly, using Eq.(7), the $\Phi_{I,J}^{P-H}$ (Eq.24) term can be written as

$$\begin{aligned} \Phi_{I,J}^{P-H} \approx & 2 \sum_{\mu,\nu} \sum_{\mathbf{r}} P_{\mu,\nu} \cdot \frac{\partial w(\mathbf{r})}{\partial \mathbf{R}_J} \left[\frac{\partial \chi_{\mu}(\mathbf{r})}{\partial \mathbf{R}_I} \hat{h}_{KS} \chi_{\nu}(\mathbf{r}) \right] \\ & + 2 \sum_{\mu,\nu} \sum_{\mathbf{r}} P_{\mu,\nu} \cdot w(\mathbf{r}) \\ & \cdot \left[\frac{\partial^2 \chi_{\mu}(\mathbf{r})}{\partial \mathbf{R}_I \partial \mathbf{R}_J} \hat{h}_{KS} \chi_{\nu}(\mathbf{r}) \right. \\ & + \frac{\partial \chi_{\mu}(\mathbf{r})}{\partial \mathbf{R}_I} \frac{d \hat{h}_{KS}}{d \vec{R}_J} \chi_{\nu}(\mathbf{r}) \\ & \left. + \frac{\partial \chi_{\mu}(\mathbf{r})}{\partial \mathbf{R}_I} \hat{h}_{KS} \frac{\partial \chi_{\nu}(\mathbf{r})}{\partial \vec{R}_J} \right]. \quad (33) \end{aligned}$$

It should be noted that, when using Gaussian basis set^{12,20,21}, only the Pulay term contains xc part need to be considered, and the \hat{h}_{KS} is replaced by \hat{v}_{xc} .

And finally, the integration form of $\Phi_{I,J}^{P-S}$ (Eq.26) is

$$\begin{aligned} \Phi_{I,J}^{P-S} \approx & 2 \sum_{\mu,\nu} \sum_{\mathbf{r}} W_{\mu,\nu} \cdot \frac{\partial w(\mathbf{r})}{\partial \mathbf{R}_J} \left[\frac{\partial \chi_{\mu}(\mathbf{r})}{\partial \mathbf{R}_I} \chi_{\nu}(\mathbf{r}) \right] \\ & + 2 \sum_{\mu,\nu} \sum_{\mathbf{r}} W_{\mu,\nu} \cdot w(\mathbf{r}) \\ & \cdot \left[\frac{\partial^2 \chi_{\mu}(\mathbf{r})}{\partial \mathbf{R}_I \partial \mathbf{R}_J} \chi_{\nu}(\mathbf{r}) + \frac{\partial \chi_{\mu}(\mathbf{r})}{\partial \mathbf{R}_I} \frac{\partial \chi_{\nu}(\mathbf{r})}{\partial \vec{R}_J} \right]. \quad (34) \end{aligned}$$

When considering moving-grid effect, the second derivative of basis function is written as,

$$\frac{\partial^2 \chi_{\mu}(\vec{r})}{\partial \vec{R}_I \partial \vec{R}_J} = \begin{cases} \nabla^2 \chi_{\mu}(\vec{r}) \delta_{I(\mu),J} & \text{if } \mathbf{r} \notin \text{atom}_J \\ -\nabla^2 \chi_{\mu}(\vec{r}) (1 - \delta_{I(\mu),J}) & \text{if } \mathbf{r} \in \text{atom}_J \end{cases} \quad (35)$$

Other Pulay terms $\Phi_{I,J}^{P-P}$ (Eq.23) and $\Phi_{I,J}^{P-W}$ (Eq.25) contains the derivatives which similar to Pulay force, so the moving-grid effect do not need to be considered as explained in Sec.II A.

III. RESULTS

The grids setting in FHI-aims is characterized by light, tight and really-tight by increasing the radial multiplier $N_{r,mult}$ and the maximum number of angular integration points $N_{ang,max}$, e.g. for hydrogen atom, the number of total integration grids is shown in Tab.I.

In Table II, we present force constants for hydrogen dimer with a local approximation for exchange and correlation (LDA parametrization of Perdew and Zunger²⁶ for the correlation energy density of the homogeneous electron gas based on the data of Ceperley and Alder²⁷). In all cases, the force constants calculations were performed for the respective equilibrium geometry, i.e., the structure obtained by relaxation (maximum force $< 10^{-4}$ eV/Å)

Hydrogen atom	$N_{r,mult}$	$N_{ang,max}$	N
light	1	302	4740
tight	2	434	14450
really-tight	2	590	19502

TABLE I. Different grid settings for the hydrogen atom.

Hessian of H ₂ (Hartree/Bohr ²)		DFPT fixed	DFPT moving	fd
$\Phi_{1x,1x}^{HF}$	light	-1.499	0.3331	0.3332
	tight	-1.499	0.3332	0.3332
	really-tight	-1.499	0.3333	0.3333
$\Phi_{1x,2x}^{HF}$	light	-0.3338	-0.3334	-0.3332
	tight	-0.3335	-0.3332	-0.3332
	really-tight	-0.3335	-0.3333	-0.3333
$\Phi_{1x,1x}^P$	light	-0.00096	-0.00092	-0.001028
	tight	-0.001184	-0.001195	-0.001185
	really-tight	-0.001188	-0.001192	-0.001189
$\Phi_{1x,2x}^P$	light	0.001242	0.001228	0.001028
	tight	0.001197	0.001197	0.001185
	really-tight	0.001195	0.001194	0.001189
$\Phi_{1x,1x}^{MP}$	light			-0.0003
	tight			-0.0001
	really-tight			0.00001
$\Phi_{1x,2x}^{MP}$	light			0.0003
	tight			0.0001
	really-tight			-0.00001

TABLE II. Hessian (Hartree/Bohr²) of H₂ molecule computed with LDA functional, tier 2 basis set.

using the exact same computational settings. In the following, a minimal basis includes the radial functions of the occupied orbitals of free atoms with noble gas configuration and quantum numbers of the additional valence functions. And additional radial functions are added to make “tier 1”, “tier 2”, and so on. See Ref.²³ for more details. Here in Table II and Table III we use tier 2 basis set.

In Table II, DFPT-fix means to use Eq.(16)-Eq.(27) as shown in Sec.II B for all the force constants and DFPT-moving means to consider moving grid effect, and by using Eq.(28)-Eq.(35) as shown in Sec.II C. To validate with DFPT result, we have also obtained vibrational frequencies with finite difference calculations, in which the Hessian was obtained via a first order finite difference expression for the forces using an atomic displacement of 0.0025 Å. Here in fd, we use Eq.(10) for Hellmann-Feynman force.

From Table II, it can be seen that (1) The diagonal part of Hellmann-Feynman term in force constant could be wrong if not considering moving grid effect, no matter which grids is using. For hydrogen, $\Phi_{1x,1x}^{HF}$ is not changed even really-tight setting grid is used. (2) The

Frequency(cm^{-1}) of H ₂	DFPT-moving	fd	Δ (DFPT-fd)
light	4173.6	4171.5	2.1
tight	4172.2	4171.5	0.7
really-tight	4172.9	4173.2	0.3

TABLE III. Frequencies (cm^{-1}) of H₂ molecule computed with LDA functional, tier 2 basis set.

Frequency(cm^{-1})		DFPT	DFPT	DFPT	fd
		fix-HF	fix-Pulay	moving	
H ₂	minimal	-3683.6	3341.2	3341.5	3341.3
	tier 1	-5603.9	4206.6	4206.5	4207.1
	tier 2	-5533.9	4172.9	4172.9	4173.2
F ₂	minimal	-152460.1	976.5	969.5	967.9
	tier 1	-152431.1	1061.2	1054.8	1055.0
	tier 2	-411634.1	1072.1	1062.8	1063.2
Cl ₂	minimal	-411634.1	676.7	476.7	475.2
	tier 1	-411600.8	738.3	565.8	563.4
	tier 2	-411600.6	737.2	564.2	561.9

TABLE IV. The moving grid effect with respect to different basis set and different element with really-tight grid and LDA functional.

non-diagonal part of Hellmann-Feynman term could be gotten using DFPT-fix scheme, by increasing the grid, the relative error could be reduced from 0.18% (light) to 0.06% (really-tight). (3) Compared with Hellmann-Feynman term, the moving-grid in Pulay term is smaller. As we use a large basis (tier 2) here, the Hellmann-Feynman term is ~ 333 times over Pulay term. And here for hydrogen, the moving-grid effect seems very small for both diagonal part and non-diagonal part in Pulay term. This is because hydrogen is a light element, and the moving-grid effect is not remarkable here, however in the following we will see the moving-grid effect is noticeable in the heavier elements. (4) The percentage of multipole correction term in total force constant is around 0.1% with light grid setting and less than 0.003% with really-tight grid setting, so it has been omitted in the following force constants calculation.

From Table III it can be seen that by considering moving-grid effect, we could get right vibrational frequency compared with finite difference method. And the absolute error reduced from $2.1 cm^{-1}$ with light setting grid to $0.3 cm^{-1}$ with really-tight grid.

In order to see the influence of different basis set and elements, we present harmonic frequencies for different dimers H₂, F₂ and Cl₂ computed with LDA functional and really-tight grid setting using three different basis set: minimal, tier1 and tier2 as described above. DFPT frequencies are computed analytically for three conditions: (1) fix-HF, consider moving-grid effect only in Pulay term; (2) fix-Pulay, consider moving-grid effect only in Hellmann-Feynman term; (3) moving, consider

	Frequency (cm^{-1})	DFPT-fix-ASR fd-screened	
		fd	screened
H ₂	minimal	3341.9	3341.9
	tier 1	4208.1	4208.3
	tier 2	4174.5	4174.5
F ₂	minimal	969.6	968.7
	tier 1	1054.9	1054.3
	tier 2	1062.9	1062.3
Cl ₂	minimal	476.6	474.9
	tier 1	565.6	564.3
	tier 2	563.9	562.7

TABLE V. The moving grid effect can be bypassed using acoustic sum rule. The DFPT results using fixed grid as well as acoustic sum rule show excellent agreement with finite-difference results. Here we use really-tight grid and LDA functional.

moving-grid effect in both Hellmann-Feynman term and Pulay term. In finite difference (fd) calculations, the force constant was also obtained via a first order finite difference expression for the forces using an atomic displacement of 0.0025 \AA , using Eq.(10) for Hellmann-Feynman force.

A detailed list of results is given in the Table IV. It can be seen that an excellent agreement between our DFPT-moving implementation and the finite-difference results. The difference between frequencies computed using the DFPT-moving method and fd method is typically less than $3 cm^{-1}$, which is acceptable, (the largest absolute error $2.4 cm^{-1}$ occurs for Cl₂ with tier 1 basis set); On the other hand, we could see the significant problem without considering moving-grid effect. (1) For DFPT-fix-Pulay, F₂ has errors of $7 cm^{-1}$ (mini), $6.4 cm^{-1}$ (tier 1) and $9.3 cm^{-1}$ (tier 2). The situation further worsens for Cl₂, which has errors of $200 cm^{-1}$ (mini), $172.5 cm^{-1}$ (tier 1) and $173.0 cm^{-1}$ (tier 2). (2) For DFPT-fix-HF, all the frequencies just go to negative which is completely wrong.

As discussed for Table II, the moving-grid effect has a much smaller influence on the non-diagonal terms of the force constant. This is because the form of non-diagonal term is similar to force calculation, which has been shown before that the moving-grid effect could be neglected if sufficient grid is used (large than 3500 per atom)²⁰. As a result, we could use DFPT-fix method to get the non-diagonal terms and then using translational invariance, which is also known as acoustic sum rule (ASR) to get the diagonal terms:

$$\frac{\partial^2 E_{tot}}{\partial R_{I\alpha} \partial R_{I\beta}} = - \sum_{J \neq I} \frac{\partial^2 E_{tot}}{\partial R_{I\alpha} \partial R_{J\beta}} \quad (36)$$

In this way, we could have right frequencies using DFPT-fix-ASR method, as shown in Tab.V. Here in finite difference calculations which labelled as fd-screened, we use Eq.(9) for Hellmann-Feynman force, and the force constant was obtained via a first order finite difference expression for the forces using an atomic displacement

of 0.0025 Å. Here we could see an excellent agreement between our DFPT-fix-ASR implementation and the finite-difference results. The difference between frequencies computed using DFPT-fix-ASR method and fd-screened method is typically less than 2 cm^{-1} , which is in good agreement, the largest absolute error 1.7 cm^{-1} occurs for Cl_2 with minimal basis set. If compare fd-screened with fd in Tab.IV, we could see difference is in all cases less than 1 cm^{-1} , which shows the moving-grid effect is indeed not necessary to Hellmann-Feynman force calculation.

IV. CONCLUSIONS

In this work, we have shown the moving-grid effect in second-order derivatives (i.e. vibrational frequencies) calculations, the formulas of moving-grid effect in Hellmann-Feynman Hessian and Pulay Hessian have been derived and implemented. In particular, we have shown the moving-grid influence with respect to the numerical parameters used in the computation, i.e. grid, basis set, elements. Also, we have demonstrated that the computed vibrational frequencies by considering moving-grid effect are essentially equal to the ones obtained from finite differences. Furthermore, we have shown by considering acoustic sum rule, the moving-grid effect could be omitted.

V. ACKNOWLEDGMENTS

The author acknowledges Professor Patrick Rinke for many inspiring discussions, and is grateful to Professor Matthias Scheffler for his generous support on this project.

¹P. Hohenberg, Physical Review **136**, B864 (1964).

- ²W. Kohn and L. J. Sham, Physical Review **140**, A1133 (1965).
³X. Gonze, Physical Review B **55**, 10337 (1997).
⁴X. Gonze and C. Lee, Phys. Rev. B **55**, 10355 (1997).
⁵S. Baroni, S. de Gironcoli, A. Dal Corso, and P. Giannozzi, Rev. Mod. Phys. **73**, 515 (2001).
⁶J. Gerratt and I. M. Mills, The Journal of Chemical Physics **49**, 1719 (1968).
⁷J. A. Pople, R. Krishnan, H. B. Schlegel, and J. S. Binkley, International Journal of Quantum Chemistry **16**, 225 (1979).
⁸C. E. Dykstra and P. G. Jasien, Chemical Physics Letters **109**, 388 (1984).
⁹M. Frisch, M. Head-Gordon, and J. Pople, Chemical Physics **141**, 189 (1990).
¹⁰C. Ochsenfeld and M. Head-Gordon, Chemical Physics Letters **270**, 399 (1997).
¹¹W. Liang, Y. Zhao, and M. Head-Gordon, The Journal of Chemical Physics **123**, 194106 (2005).
¹²B. G. Johnson, P. M. W. Gill, and J. a. Pople, The Journal of Chemical Physics **98**, 5612 (1993).
¹³X. Andrade, D. Strubbe, U. De Giovannini, A. H. Larsen, M. J. T. Oliveira, J. Alberdi-Rodriguez, A. Varas, I. Theophilou, N. Helbig, M. J. Verstraete, L. Stella, F. Nogueira, A. Aspuru-Guzik, A. Castro, M. A. L. Marques, and A. Rubio, Phys. Chem. Chem. Phys. **17**, 31371 (2015).
¹⁴J. M. Soler, E. Artacho, J. D. Gale, A. García, J. Junquera, P. Ordejón, and D. Sánchez-Portal, J. Phys. Condens. Matter **14**, 2745 (2002).
¹⁵C. Satoko, Chem. Phys. Lett. **83**, 111 (1981).
¹⁶A. D. Becke, The Journal of Chemical Physics **88**, 2547 (1988).
¹⁷B. Delley, The Journal of Chemical Physics **94**, 7245 (1991).
¹⁸B. G. Johnson, M. J. Frisch, W. Avenue, and N. Haven, **216**, 133 (1993).
¹⁹B. G. Johnson and M. J. Fisch, The Journal of Chemical Physics **100**, 7429 (1994).
²⁰J. Baker, J. Andzelm, A. Scheiner, and B. Delley, The Journal of Chemical Physics **101**, 8894 (1994).
²¹M. Malagoli and J. Baker, The Journal of Chemical Physics **119**, 12763 (2003).
²²H. Shang, C. Carbogno, P. Rinke, and M. Scheffler, Computer Physics Communications **215**, 26 (2017).
²³V. Blum, R. Gehrke, F. Hanke, P. Havu, V. Havu, X. Ren, K. Reuter, and M. Scheffler, Comput. Phys. Commun. **180**, 2175 (2009).
²⁴B. Delley, J. Chem. Phys. **92**, 508 (1990).
²⁵B. Delley, Journal of Computational Chemistry **17**, 1152 (1996).
²⁶J. Perdew and A. Zunger, Phys. Rev. B **23**, 5048 (1981).
²⁷D. Ceperley and B. Alder, Phys. Rev. Lett. **45**, 566 (1980).